OMTN, Volume *34*

Supplemental information

Efficient shRNA-based knockdown of multiple target genes for cell therapy using a chimeric miRNA cluster platform

Matteo Rossi, Mikhail Steklov, Fanny Huberty, Thuy Nguyen, Jérôme Marijsse, Céline Jacques-Hespel, Paul Najm, Caroline Lonez, and Eytan Breman

Figure S1

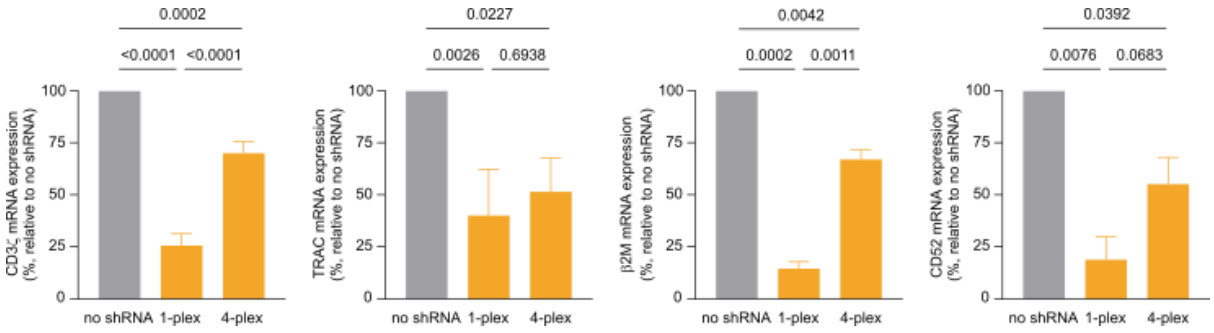

Figure S1. Rationale for the building of a multiplex miRNA-based shRNA platform
Effect on KD efficiency of the use of the same scaffold in tandem repeats. The KD efficiency of four different shGuide sequences was compared in a single miR196a-2 scaffold and in the context of a 4-plex made of repeats of the miR196a-2 scaffold transduced in CAR T-cells. KD efficiency was measured by qPCR relative to a control without shRNA, using validated shRNA-derived sequences. Bars represent mean ± standard deviation (SD) for three independent biological replicates from different PBMC donors.

Figure S2

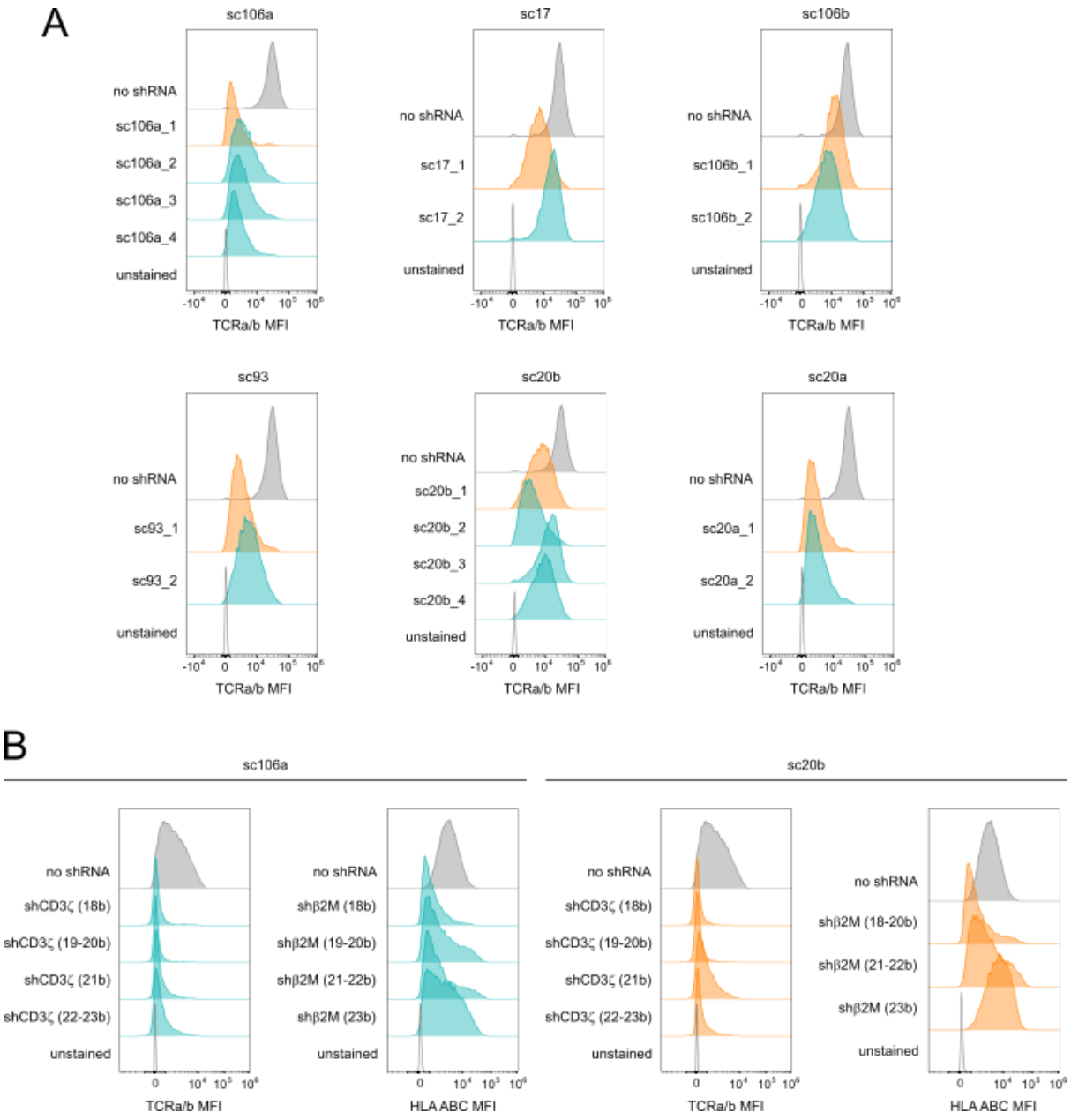

Figure S2. Identification of the optimal scaffold and shGuide sequence length

(A) Representative FACS histograms from one PBMC donor for the KD efficiencies of a shGuide sequence against the T-cell receptor (TCR) component CD3ζ, obtained from the sequential deletions of each of the candidate scaffolds, measured in CAR T-cells as surface expression of TCRa/b. The orange curves correspond to the scaffold lengths ultimately chosen for further experiments. (B) Representative FACS histograms from one PBMC donor for the KD efficiencies of shGuide sequences spanning between 18 and 25 bases against CD3ζ and the HLA class I component β2M in the context of two different scaffolds (sc106a and sc20b), measured in CAR T-cells as surface expression of TCRa/b and HLA ABC respectively. The orange curves correspond to the shGuide sequence lengths ultimately chosen for further experiments.

Figure S3

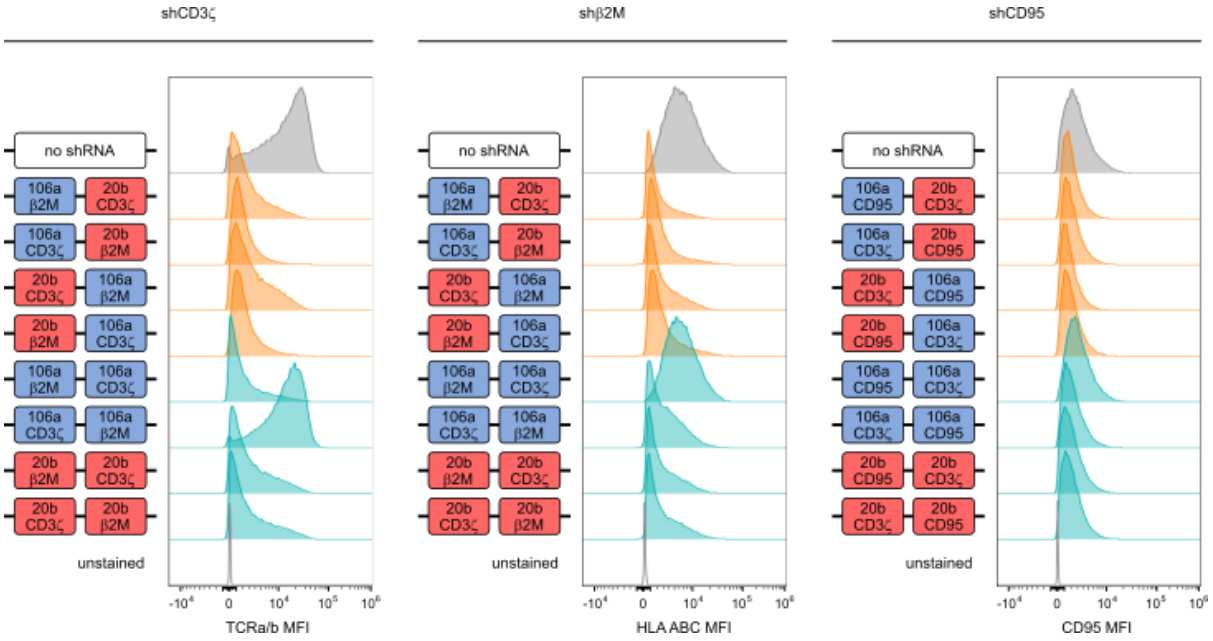

Figure S3. Effect of scaffold combination on KD efficiency in a 2-plex miRNA platform
Results of two different approaches followed to build a chimeric cluster: combining two different scaffold or replicating same scaffold multiple times. Combinations of sc106b and sc20b as well as repetitions of either sc106a or sc20b were tested in a 2-plex with validated shGuide sequences against CD3ζ, β2M and CD95. Different configurations of the 2-plex were tested, alternating the position of the scaffolds and of the shGuide sequences. Representative FACS histograms from one PBMC donor are depicted for the KD efficiencies of TCRa/b, HLA ABC and CD95, respectively, in CAR T-cells transduced with the 2-plex and with a no shRNA control.

Figure S4

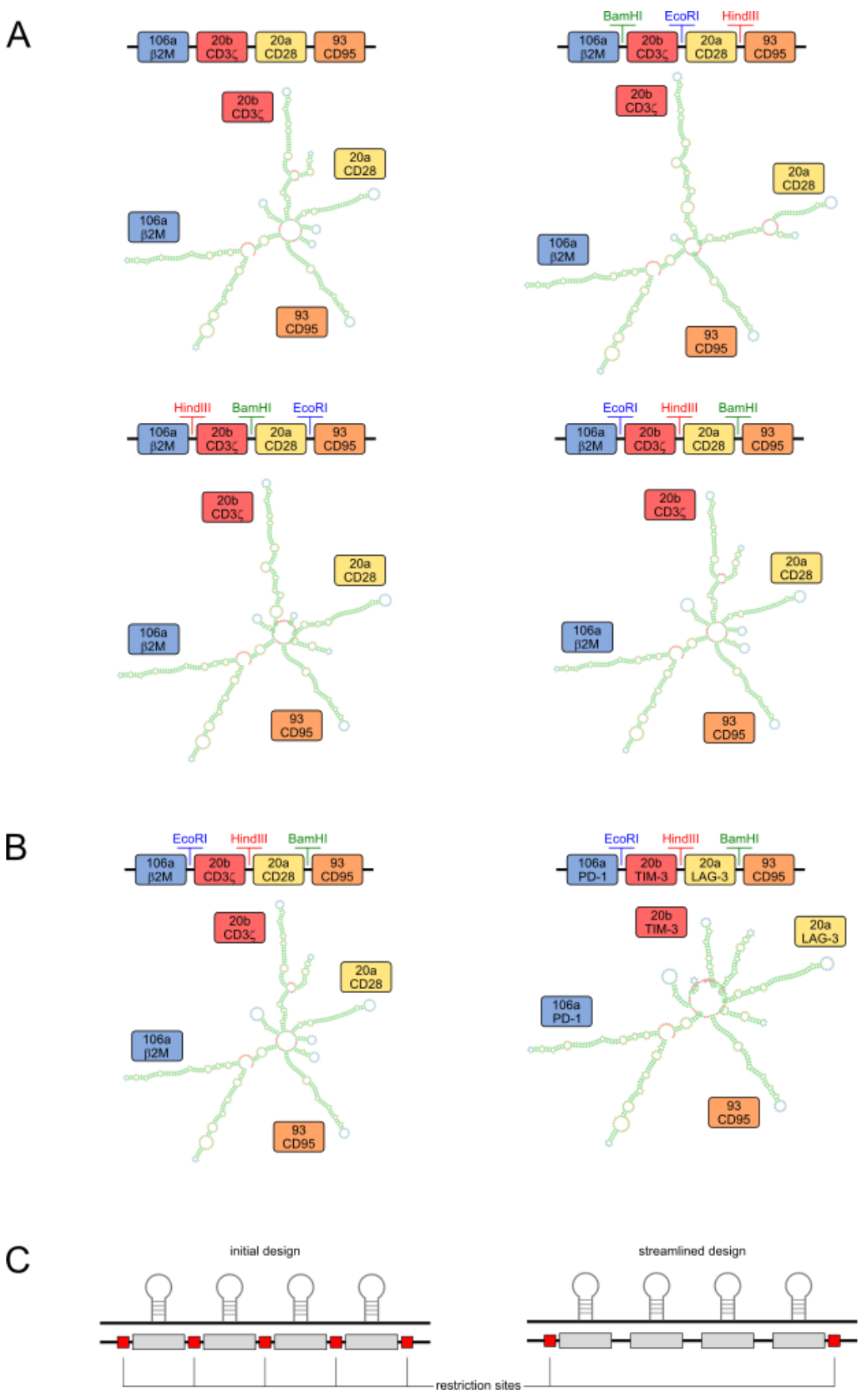
A
106a β2M
20b CD3ζ
20a CD28
93 CD95
BamHI
EcoRI
HindIII
B
106a PD-1
20b TIM-3
20a LAG-3
C
initial design
streamlined design
restriction sites

Figure S4. Effect of restriction sites between the scaffolds on the secondary structure of the chimeric clusters

(A) Restriction sites for BamHI, EcoRI and HindIII were inserted between the scaffolds in a sc106a – sc20b – sc20a – sc93 chimeric cluster and were shifted along to achieve all three possible combinations, without modifying the position of the scaffolds or of the shGuide sequences within the scaffolds. The resulting sequences were analyzed *in silico* using the RNAfold secondary structure prediction tool. The RNA secondary structures depicted for each cluster represent the most stable configuration based on minimum free energy prediction. (B) In a sc106a – sc20b – sc20a – sc93 chimeric cluster, the scaffolds and the restriction sites between the scaffolds were maintained in fixed positions, but the shGuide sequences within the scaffold were changed. The resulting sequences were analyzed *in silico* using the RNAfold secondary structure prediction tool. The RNA secondary structures depicted for each cluster represent the most stable configuration based on minimum free energy prediction. (C) Schematic representation of the 4-plex design with or without restriction sites between the scaffolds.

Figure S5

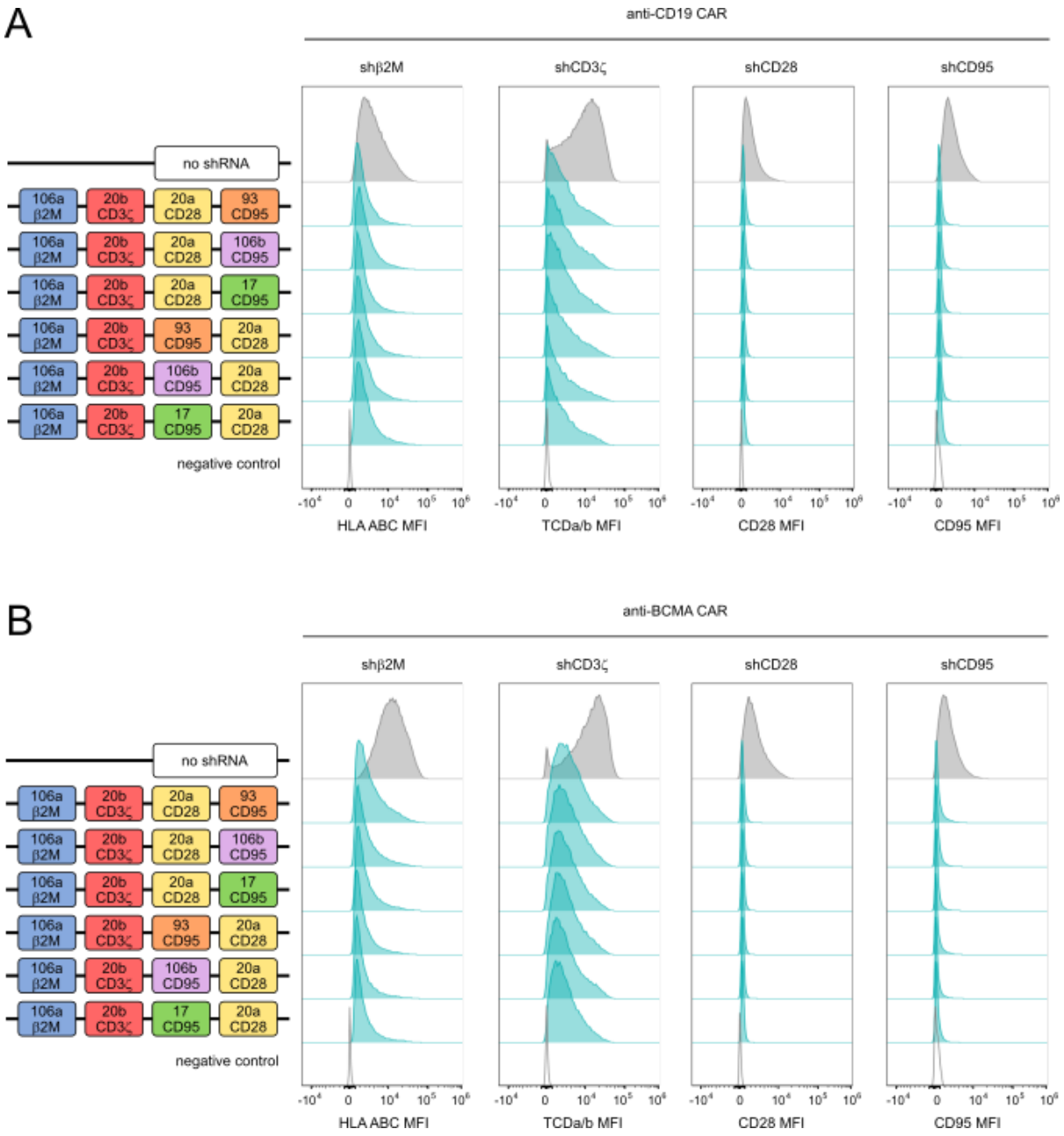

Figure S5. Selection of scaffolds for the expansion of the miRNA-based shRNA platform to a 4-plex
Starting with the sc106a – sc20b 2-plex as a basis, the platform was expanded into a 4-plex by the addition of two extra scaffolds. In a first cluster design, sc20a was added in third position, and sc93, sc106b or sc17 in fourth position. In a second cluster design, sc93, sc106b or sc17 were added in third position and sc20a in fourth position. Each position carried a different validated shGuide sequence (β2M, CD3ζ, CD28 and CD95). Representative FACS histograms from one PBMC donor are depicted for the KD efficiency of TCRa/b, HLA ABC, CD28 and CD95, respectively, in CAR T-cells transduced with the 4-plex constructs or with a no shRNA control. The different 4-plex combinations were tested in the context of both an anti- CD19 CAR (A) and an anti-BCMA CAR (B).

Figure S6

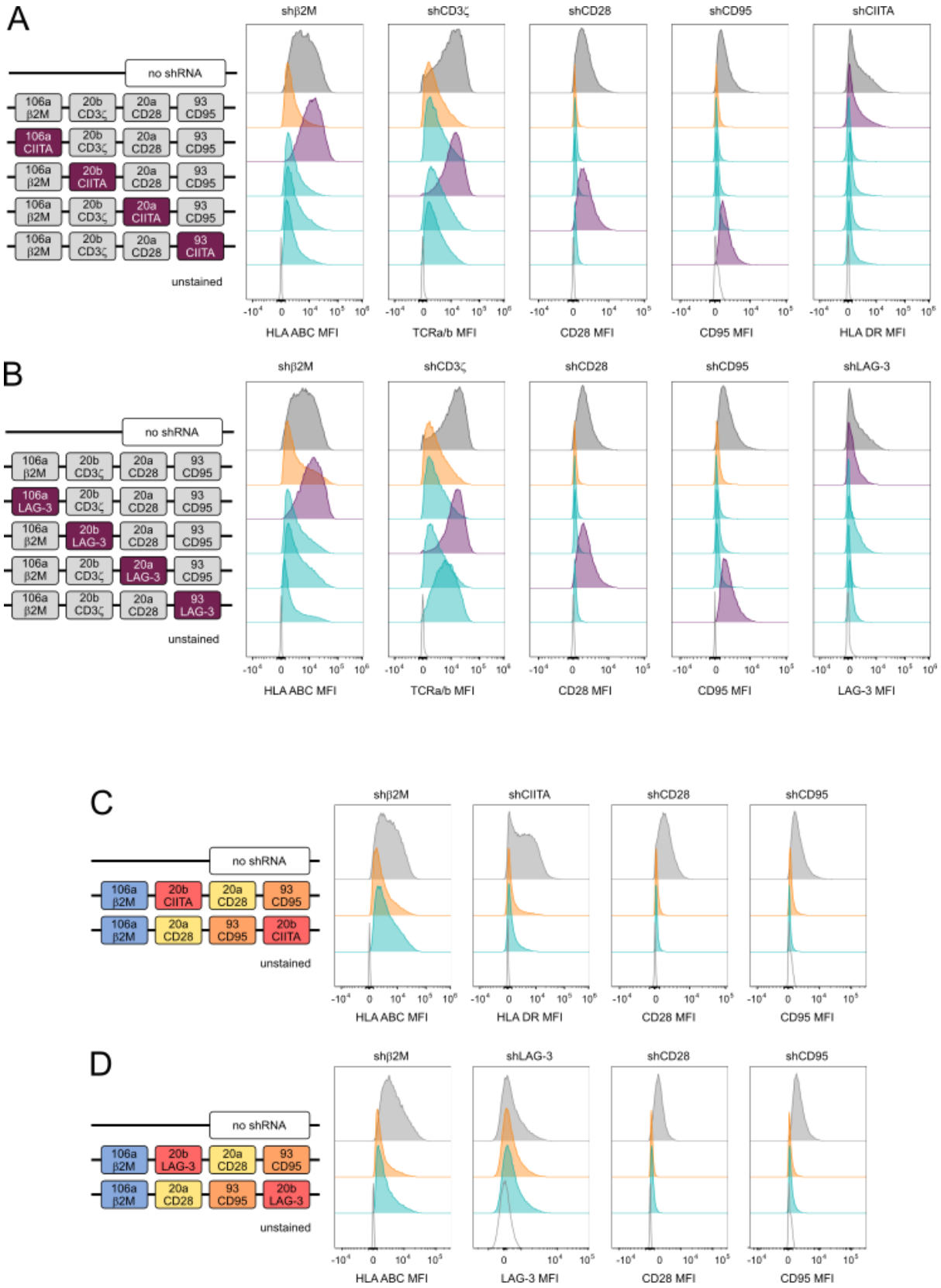
A
shβ2M
shCD3ζ
shCD28
shCD95
shCIITA
no shRNA
106a β2M
20b CD3ζ
20a CD28
93 CD95
106a CIITA
20b CIITA
20a CIITA
93 CIITA
unstained
HLA ABC MFI
TCRa/b MFI
CD28 MFI
CD95 MFI
HLA DR MFI
B
shβ2M
shCD3ζ
shCD28
shCD95
shLAG-3
no shRNA
106a LAG-3
20b LAG-3
20a LAG-3
93 LAG-3
unstained
HLA ABC MFI
TCRa/b MFI
CD28 MFI
CD95 MFI
LAG-3 MFI
C
shβ2M
shCIITA
shCD28
shCD95
no shRNA
unstained
HLA ABC MFI
HLA DR MFI
CD28 MFI
CD95 MFI
D
shβ2M
shLAG-3
shCD28
shCD95
no shRNA
unstained
HLA ABC MFI
LAG-3 MFI
CD28 MFI
CD95 MFI

Figure S6. Assessing the plug-and-play capability of the 4-plex miRNA-based shRNA platform
To test the plug-and-play capability of the 4-plex and its stability irrespective of the target, a fifth and sixth shGuide sequence were substituted in each position in the sc106a – sc20b – sc20a – sc93 cluster carrying validated shGuide sequences against β2m, CD3ζ, CD28 and CD95, in the context of an anti-CD19 CAR. Validated shRNAs-derived sequences against CIITA (A), a key coregulator that controls expression of HLA class II genes, and LAG-3 (B) were used for the purpose. Representative FACS histograms from one PBMC donor are depicted for the KD efficiency of all targets, including HLA DR, one of the main MHC II proteins, as proxy for CIITA and the immune checkpoint LAG-3, in CAR T-cells transduced with the 4-plex constructs or with a no shRNA control. As LAG-3 is expressed at low levels in resting T-cells, but is induced following T-cell activation, surface LAG-3 expression was assessed upon co-culture for 24h with NALM-6, a human pre-B ALL cell line positive for CD19. As a marked loss in KD efficiency was observed when the shGuide sequence against LAG-3 was in sc20b, to determine whether this is due to a positional effect of this scaffold, a construct with sc20b in position 4 (sc106a – sc20a – sc93 – sc20b) was tested in comparison with the original cluster with sc20b in position 2 (sc106a – sc20b – sc20a – sc93) and a no shRNA control. The comparison was made with both CIITA (C) and LAG-3 (D) shGuide sequences. Representative FACS histograms from one PBMC donor are depicted for the KD efficiencies of HLA DR and LAG-3, the latter upon co-culture for 24h with NALM-6 cells.

Figure S7

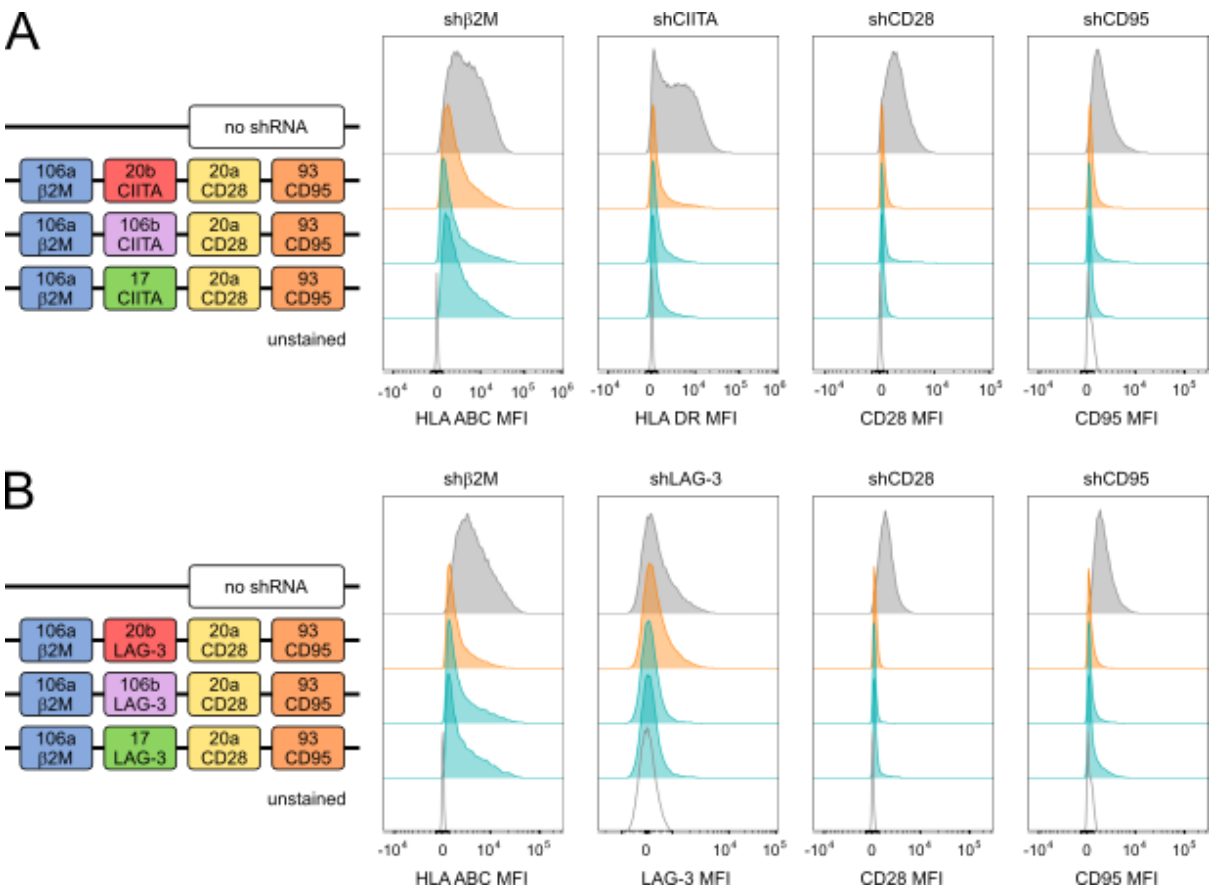

Figure S7. Testing of an updated version of the 4-plex miRNA-based shRNA platform with true plug-and-play capability

As an alternative to the unstable sc106a – sc20a – sc93 – sc20b configuration of the 4-plex, different designs were tested, in which sc20b was substituted by sc106b or sc17, in the context of an anti-CD19 CAR. The clusters carried validated shGuide sequences against β2M in position 1, CD28 in position 3 and CD95 in position 4. In position 2, where sc20b originally laid, validated shGuide sequences against CIITA (A) and LAG-3 (B) were introduced. Representative FACS histograms from one PBMC donor are depicted for the KD efficiency of HLA ABC, HLA DR (respectively controlled by β2M and CIITA), LAG-3, CD28 and CD95. As LAG-3 is expressed at low levels in resting T-cells, but is induced following T-cell activation, surface LAG-3 expression was assessed upon co-culture for 24h with NALM-6, a human pre-B ALL cell line positive for CD19.

Table S1. Full sequences of the miRNA scaffolds depicted in Figure 2A and 2B.

Table S2 Absolute MFI of the no shRNA control samples for the flow cytometry markers.